Research Square

Preprints are preliminary reports that have not undergone peer review.
They should not be considered conclusive, used to inform clinical practice,
or referenced by the media as validated information.

Groundwater Potential Assessment Using Ann-Rks Machine Learning Based Models in Part of Aule Community, Akure, Nigeria

Timilehin Damilare Akande

akandedamilare.t@gmail.com

Federal University of Technology

Olaoluwa James Akintorinwa

Federal University of Technology

Research Article

Keywords: Groundwater Potential Mapping, Artificial Neural Network (ANN), Random Kitchen Sinks (RKS), Vertical Electrical Sounding (VES), Remote Sensing and Geographic Information System (GIS)

Posted Date: November 13th, 2026

DOI: https://doi.org/10.21203/rs.3.rs-10897801/v1

License: This work is licensed under a Creative Commons Attribution 4.0 International License.
Read Full License

Additional Declarations: No competing interests reported.

GROUNDWATER POTENTIAL ASSESSMENT USING ANN-RKS MACHINE LEARNING BASED MODELS IN PART OF AULE COMMUNITY, AKURE, NIGERIA

Authors: Akande, Timilehin Damilare and Akintorinwa, Olaoluwa James

Department of Applied Geophysics, Federal University of Technology, Akure.

Corresponding Author's Mail: akandedamilare.t@gmail.com

Abstract

This study adopted an integrated approach combining hydrogeological, geophysical, and machine learning techniques to evaluate groundwater potential in Aule Community, Akure, Ondo State, Southwestern Nigeria. Remote sensing data, particularly the ASTER Global Digital Elevation Model (DEM), were processed in ArcMap 10.8.2 to derive key terrain conditioning factors such as slope and aspect, which influence surface runoff, infiltration, and groundwater recharge. The geophysical investigation involved electrical resistivity surveys using the Schlumberger array configuration, with 105 Vertical Electrical Sounding (VES) stations acquired across the study area. Interpretation of the VES data delineated five subsurface geoelectric layers: topsoil, lateritic layer, weathered layer, partially weathered or fractured basement, and fresh basement bedrock, providing detailed insight into aquifer geometry and subsurface conditions. These geoelectric and hydrogeological parameters were integrated as predictor variables within a supervised machine learning framework. A dataset comprising 40 matched well–VES control points were used for model training and validation, with hand-dug well measurements serving as the target variable. Two predictive models were developed: a conventional Artificial Neural Network (ANN) and an enhanced ANN integrated with Random Kitchen Sinks (ANN-RKS) to improve nonlinear feature representation. Using 5-fold cross-validation, the ANN-RKS model outperformed the standard ANN, achieving MAE = 0.056, MSE = 0.006, RMSE = 0.078, and R^2 = 0.910, compared to MAE = 0.082, MSE = 0.012, RMSE = 0.109, and R^2 = 0.801 for the ANN model. The optimized ANN-RKS outputs were subsequently spatially interpolated within a GIS environment to generate a detailed groundwater potential map of the study area.

Keywords: Groundwater Potential Mapping; Artificial Neural Network (ANN); Random Kitchen Sinks (RKS); Vertical Electrical Sounding (VES); Remote Sensing and Geographic Information System (GIS).

1. Introduction

Groundwater is one of the most important natural resources supporting domestic, agricultural, and industrial activities worldwide. It serves as a primary source of drinking water for billions of people, particularly in regions where surface water is scarce, unreliable, or seasonal [39]. Compared to surface water, groundwater is generally less susceptible to contamination and therefore provides a more dependable source of potable water. In agriculture, groundwater contributes significantly to global food security, supplying nearly 40% of irrigation needs, especially in arid and semi-arid regions where dependence on groundwater is high [40]. Increasing climate variability, irregular rainfall patterns, and the growing demand for food have further intensified reliance on groundwater resources. Industries including power generation, pharmaceuticals, textiles, and food processing also depend heavily on groundwater because of its naturally filtered quality and suitability for industrial applications [12]. However, excessive abstraction, poor management practices, and environmental pressures have resulted in groundwater depletion, land subsidence, and declining water quality in many regions. These challenges are further aggravated by climate change, rapid urbanization, and industrial pollution, highlighting the urgent need for effective groundwater assessment and sustainable management strategies [32].

Groundwater potential assessment is essential for understanding the availability, distribution, and sustainability of groundwater resources. As global demand for water continues to increase due to population growth, urban expansion, and climate change, accurate evaluation of groundwater potential has become increasingly important for ensuring long-term water security [28]. Reliable assessments support sustainable extraction practices, help prevent over-exploitation of aquifers, and reduce environmental problems such as land subsidence and saltwater intrusion [41]. Groundwater also serves as a critical reserve during drought periods, particularly in water-stressed regions, making its assessment crucial for climate resilience. In the agricultural sector, groundwater potential evaluation supports irrigation planning and sustainable food production while minimizing pressure on aquifer systems [61]. Furthermore, such assessments assist policymakers in regulating groundwater development projects and ensuring equitable allocation of water resources among domestic, agricultural, and industrial users. The identification of groundwater recharge zones through potential mapping also enables the implementation of measures such as afforestation and Managed Aquifer Recharge (MAR) to improve groundwater replenishment. Recent advancements in remote sensing, Geographic Information Systems (GIS), and Machine Learning (ML) have significantly enhanced groundwater potential assessment by improving prediction accuracy and supporting more informed decision-making processes [53].

Despite their widespread application, conventional groundwater assessment methods face several limitations. Traditional approaches, including hydrogeological surveys, geophysical investigations, and analytical or numerical models, often require extensive field data, substantial financial resources, and considerable time investments [44].

Groundwater studies typically depend on information such as borehole logs, aquifer characteristics, recharge measurements, and long-term monitoring records. However, in many developing countries, these datasets are often limited, outdated, or geographically incomplete, reducing the effectiveness of traditional modeling approaches [25]. Additionally, methods such as drilling and continuous monitoring are expensive and labor-intensive.

Another major limitation of conventional techniques is their inability to adequately represent the complex and non-linear interactions among geological, hydrological, climatic, and anthropogenic factors influencing groundwater systems [62]. Numerical models frequently rely on deterministic assumptions that oversimplify aquifer heterogeneity and fail to capture natural variability [60]. Similarly, geophysical methods such as electrical resistivity and seismic surveys, although valuable for subsurface characterization, are often constrained by resolution limitations, environmental interference, and interpretation uncertainties [4]. Traditional approaches also struggle to integrate diverse datasets, including geology, soil characteristics, land use patterns, climatic variables, and human activities, into a unified predictive framework [50]. Consequently, they often produce static representations of groundwater conditions that cannot adequately capture long-term changes caused by droughts, excessive abstraction, or land-use transformations [1]. Their predictive performance is particularly limited in complex hydrogeological environments such as fractured and karst aquifers, where groundwater flow patterns are highly heterogeneous and difficult to model accurately [21].

To overcome these limitations, Machine Learning (ML) techniques have emerged as powerful alternatives for groundwater potential assessment. ML models are capable of analyzing large, multidimensional datasets and identifying hidden relationships that traditional methods may overlook [18]. Among these techniques, Artificial Neural Networks (ANN) and Random Kitchen Sinks (RKS) have gained significant attention because of their ability to model complex, non-linear groundwater processes effectively. ANN, which is inspired by the structure and functioning of the human brain, can learn intricate relationships among variables such as rainfall, soil properties, topography, geology, and land use without requiring predefined assumptions about these relationships [22]. Through its multilayer architecture, ANN can capture both linear and non-linear patterns, making it highly effective for predicting groundwater recharge, water table fluctuations, and aquifer storage dynamics [60]. Research has consistently demonstrated that ANN-based models outperform conventional statistical and regression approaches in groundwater prediction tasks [37]. Furthermore, ANN can integrate data from multiple sources, including remote sensing imagery, climatic records, and geological surveys, thereby improving predictive performance.

However, ANN models are not without challenges. They often require large training datasets, involve high computational costs, and are frequently criticized for their lack of interpretability due to their “black-box” nature [45]. To address these challenges,

researchers have increasingly adopted Random Kitchen Sinks (RKS), a randomized feature-mapping technique designed to improve computational efficiency while maintaining predictive accuracy [30]. Unlike ANN, which depends on iterative weight optimization through backpropagation, RKS transforms input data into a higher-dimensional feature space using random basis functions, allowing complex non-linear relationships to be modeled through simpler linear regression techniques [14]. RKS offers advantages such as faster training, lower computational requirements, and reduced susceptibility to overfitting, making it particularly suitable for groundwater studies involving limited datasets [6].

The integration of ANN and RKS with GIS and remote sensing technologies has further enhanced groundwater potential mapping by enabling the production of high-resolution spatial predictions that support effective water resource management [53]. These models can identify areas vulnerable to groundwater depletion, predict future trends, and locate suitable recharge zones for sustainable aquifer management [9]. Although challenges related to data quality, model interpretability, and parameter optimization remain, ongoing research into hybrid ML approaches is improving the robustness and reliability of groundwater predictions [48, 11]. Overall, ANN and RKS represent significant advancements in groundwater potential assessment, offering improved accuracy, computational efficiency, and decision-support capabilities essential for sustainable groundwater management and long-term water security.

Groundwater remains a critical resource for domestic, agricultural, and industrial activities; however, its effective management is hindered by the complex and non-linear interactions among geological, hydrological, soil, and climatic factors that influence its occurrence and distribution. As highlighted earlier, conventional groundwater assessment methods often fail to adequately capture these complexities, leading to inaccurate predictions and inefficient resource management. Although studies such as Olatokunbo-Ojo and Akintorinwa [34] provided valuable insights into groundwater conditions within the Aule Area using electrical resistivity techniques, their findings were limited by the provision of only one-dimensional subsurface information, which could not fully represent the area's complex geological framework. To address these limitations, this study proposes the integration of Artificial Neural Networks (ANN) and Random Kitchen Sinks (RKS), combining the powerful non-linear learning capability of ANN with the computational efficiency and feature approximation strength of RKS. By leveraging multi-source datasets and advanced machine learning techniques, the proposed ANN-RKS framework is expected to improve the accuracy and reliability of groundwater potential assessment. Ultimately, the study seeks to contribute to sustainable groundwater management, reduce the risks associated with water scarcity, and support effective planning for irrigation, water supply, and long-term resource development in the face of increasing environmental and climatic pressures.

2. Materials and Methods

2.1 Study Area

The study area is located within Akure metropolis in Southwestern Nigeria (Fig. 1) and lies within UTM Zone 31N, with coordinates ranging approximately from 735,000 - 738,000 Easting and 803500–805500 Northing. The area is highly accessible through a well-developed transportation network, with Ilesha Garage Road serving as the major access route, supported by several minor roads and footpaths connecting different sections of the metropolis. This extensive road network facilitates movement within the area and provides easy access to key locations, making the area suitable for field investigations and groundwater exploration studies.

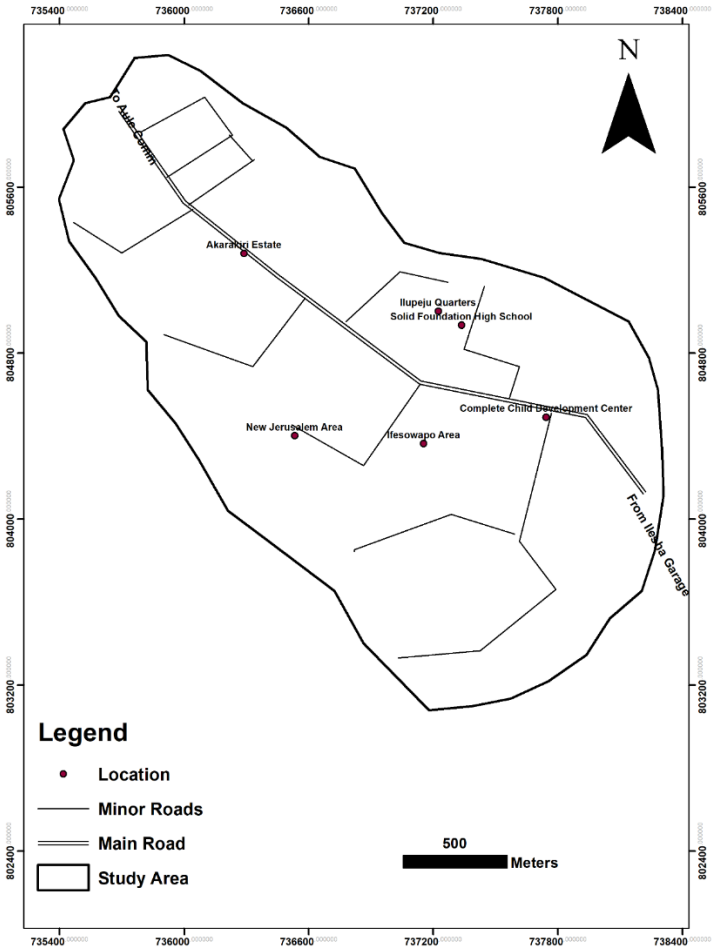


Fig. 1: Location Map of the Study Area

2.2 Geology of the Study Area

The study area is predominantly underlain by migmatite gneiss, as confirmed by both geological mapping and field observations (Fig. 2). This rock formation significantly influences the hydrogeological and geotechnical characteristics of the area, particularly

groundwater occurrence and movement. Migmatite gneiss is a metamorphic rock formed through partial melting and recrystallization of pre-existing gneiss under intense metamorphic conditions [42]. It is characterized by a distinct banded structure consisting of alternating light and dark mineral layers. The light-colored bands are mainly composed of quartz, feldspar (orthoclase and plagioclase), and muscovite, while the dark bands contain minerals such as biotite and hornblende. Granitic veins and pockets formed during partial melting are also commonly present within the rock mass.

The rock exhibits coarse- to medium-grained textures with both foliated and non-foliated characteristics resulting from the combination of gneissic and granitic components. Structurally, the migmatite gneiss displays evidence of intense tectonic activities, including folding, faulting, and shearing, which reflect the metamorphic and deformational processes responsible for its formation [19]. Similar geological features, such as banding, foliation, and granitic intrusions associated with partial melting, have been reported in migmatite gneiss outcrops within the Ibadan Schist Belt of southwestern Nigeria [15]. These structural features are important because they enhance secondary porosity and permeability, thereby influencing groundwater storage and flow within the basement complex terrain.

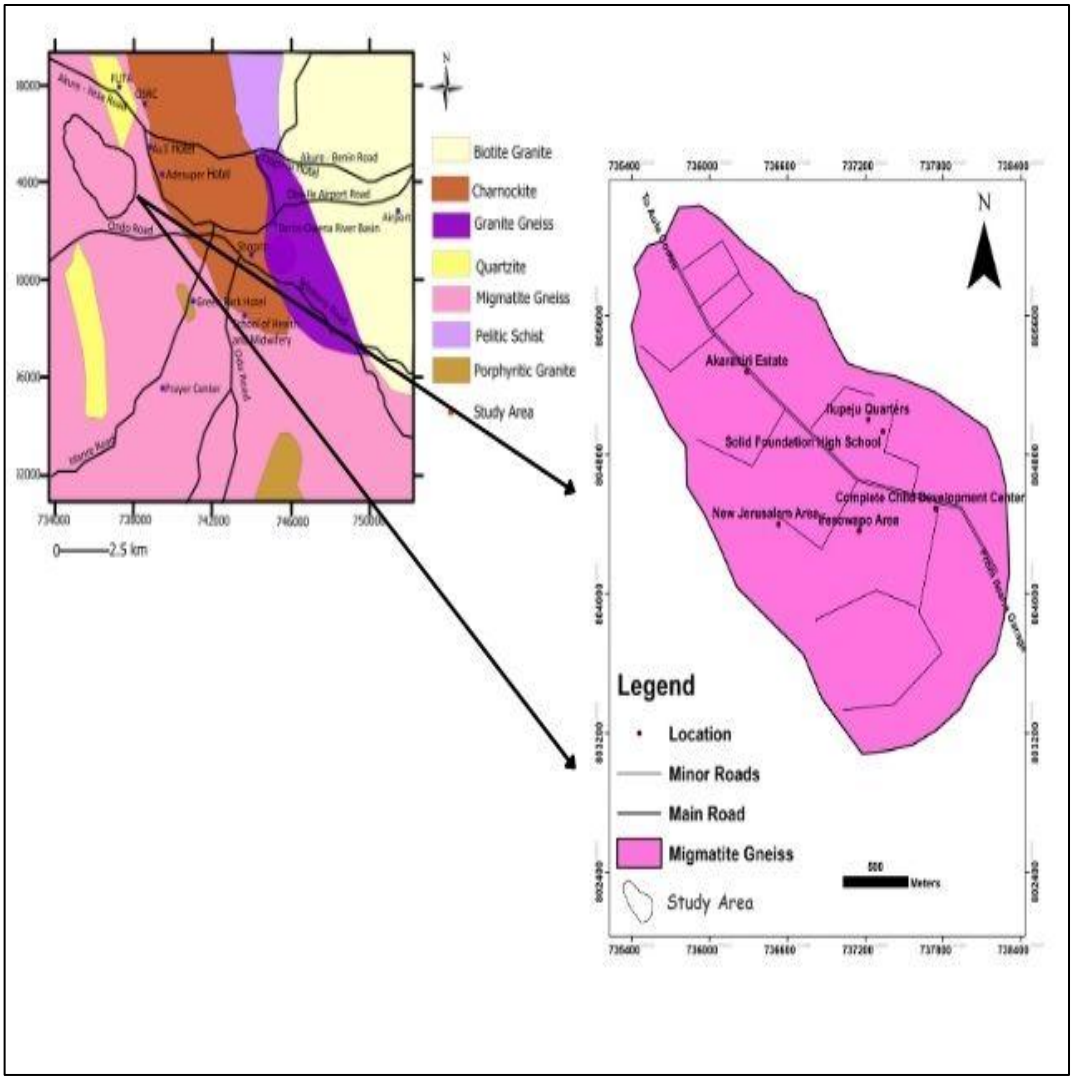


Fig. 2: Geological Map of Akure showing the Study Area (Modified after Falowo *et al.* [13])

2.3 Data Sources

2.3.1 Remote Sensing Data

A Digital Elevation Model (DEM) of the study area was obtained from the ASTER Global Digital Elevation Model (ASTER GDEM) database (https://asterweb.jpl.nasa.gov/gdem.asp). The DEM served as the primary topographic dataset for the study and was processed within a Geographic Information System (GIS) environment to derive slope and aspect maps of the area. The slope map was used to characterize terrain steepness and its influence on runoff and groundwater infiltration, while the aspect map provided information on slope orientation, which affects surface water movement, evapotranspiration, and groundwater recharge patterns. These derived thematic layers were subsequently incorporated into the groundwater potential assessment and mapping process.

2.3.2 Geophysical Data and Hydrogeological Investigation

A geoelectrical survey was conducted using the Vertical Electrical Sounding (VES) technique with the Schlumberger electrode configuration. A total of 105 VES stations were established across the study area to ensure adequate spatial coverage (Fig. 3). Measurements of apparent resistivity were obtained by progressively increasing the current electrode spacing about a fixed center point, with a maximum half-current electrode spacing (AB/2) of 150 m. The acquired VES data were processed through both qualitative and quantitative interpretation. Qualitative interpretation involved visual examination of the sounding curves to identify subsurface layering characteristics (Fig. 4), while quantitative interpretation employed partial curve matching to obtain preliminary layer resistivity and thickness values, Further interpretation was performed to determine the curve types (Fig. 5). These initial parameters were subsequently refined through one-dimensional computer modeling using the WINRESIST 2.0 software, producing the final geoelectric parameters used for further analysis Table 1.

To validate the groundwater potential assessment, a hydrogeological investigation was also carried out using 40 selected hand-dug wells distributed across the study area (Fig. 3). Measurements of water column levels and total well depths were obtained from the selected wells during fieldwork. The hydrogeological data provided valuable information on groundwater conditions within the area and served as reference data for validating the groundwater potential maps generated from the geoelectrical and geospatial analyses.

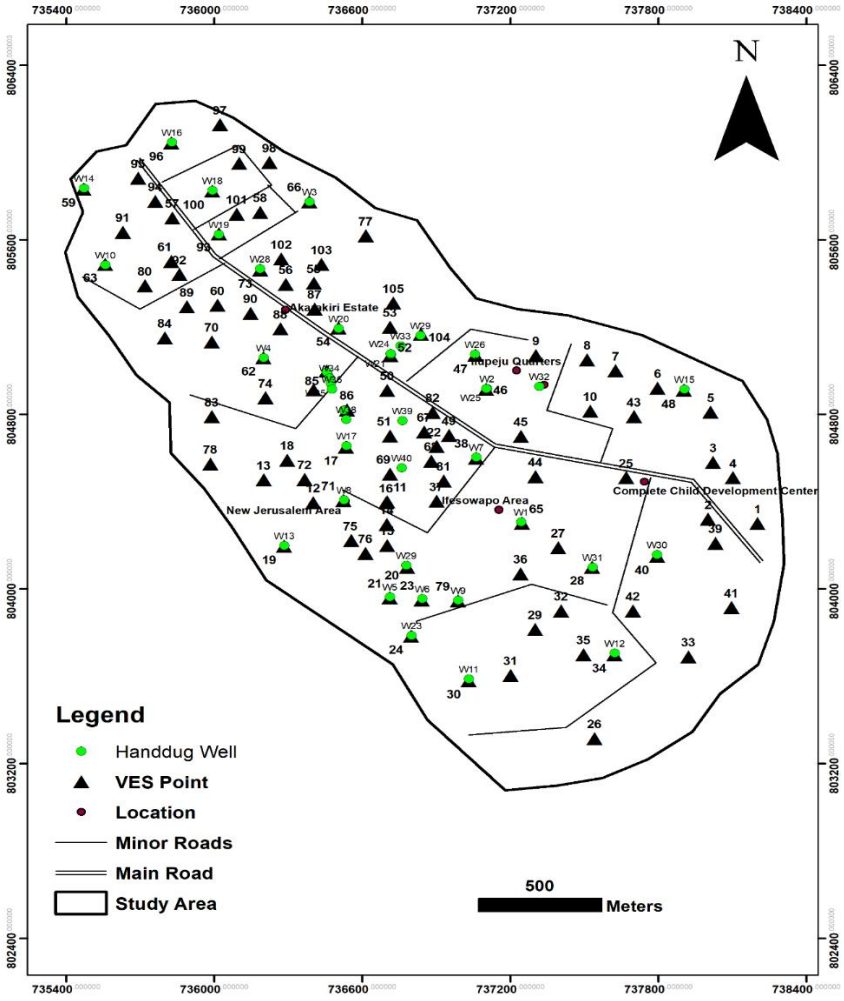
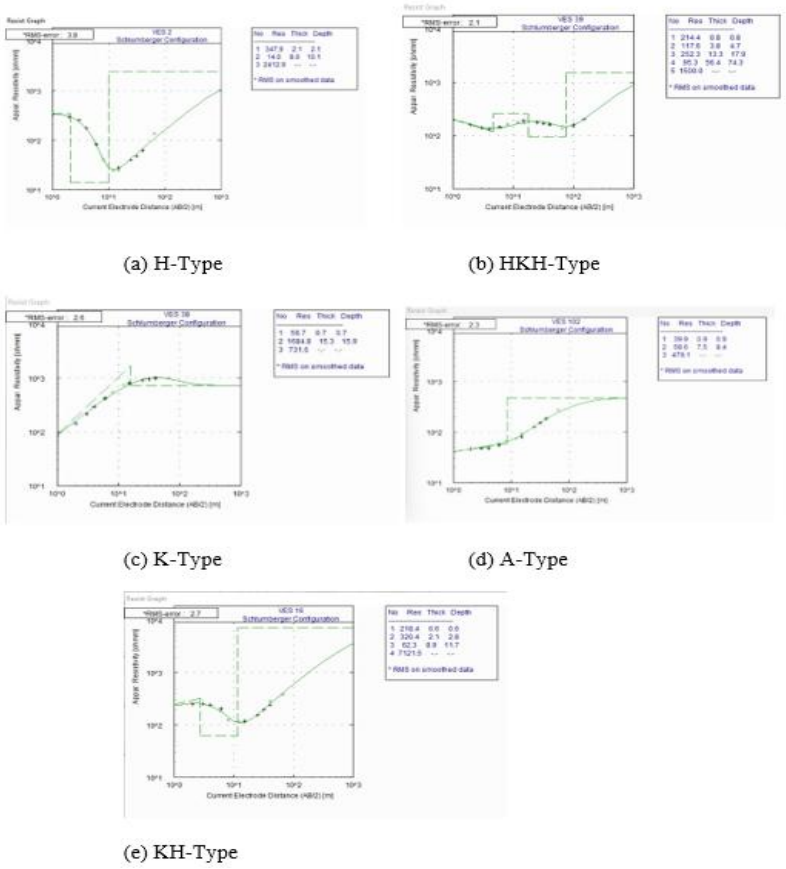


Fig. 3: Data Acquisition Map of the Study Area



(a) H-Type (b) HKH-Type

(c) K-Type (d) A-Type

(e) KH-Type

Fig. 4: Depth Sounding Curves obtained in the Study Area

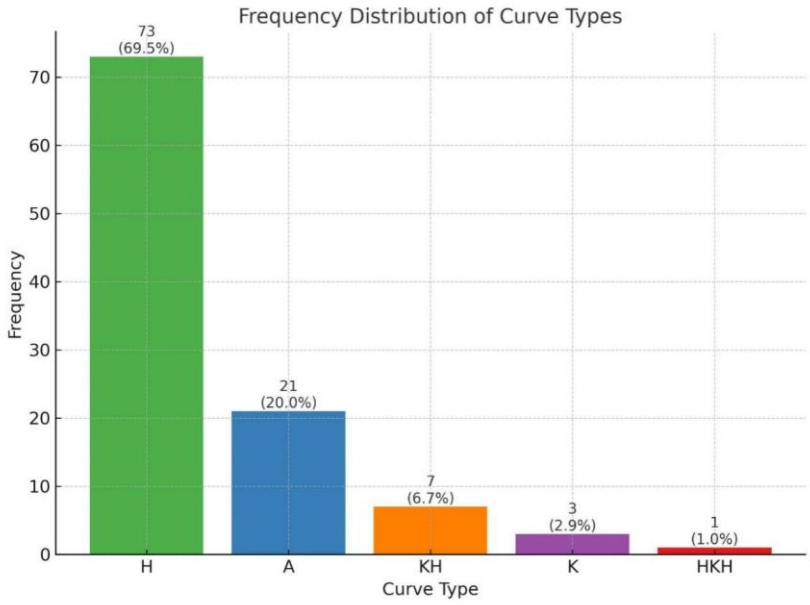


Fig. 5: Curve Type Occurrence in the Study Area

Table 1 shows a summary of the interpreted geoelectric result from some of the VES data.

VES No.	Layers	Apparent Resistivity (ohm-m)	Layer Thickness (m)	Layer Depth (m)	Lithology	Type Curve
1	1 2 3 4	20 44 11 1730	0.5 1.4 7.3 -	0.5 1.9 9.2 -	Top soil Weathered layer Weathered layer Basement Rock	KH
2	1 2 3	347 14 2412	2.1 8.0 -	2.1 10.1 -	Top soil Weathered layer Basement Rock	H
72	1 2 3	120 85 8951	0.8 6.7 -	0.8 7.5 -	Top soil Weathered layer Basement Rock	H
73	1 2 3 4	137 866 117 13098	1.7 4.3 5.9 -	1.7 6.0 11.9 -	Top soil Lateritic layer Weathered layer Basement Rock	KH
74	1 2 3	82 371 2526	3.8 40.4 -	3.8 44.2 -	Top soil Weathered layer Basement Rock	A
88	1 2 3	69 643 439	3.5 3.4 -	1.0 6.9 -	Top soil Partly weathered/Fractured basement	K

					Basement Rock	
89	1 2 3	70 42 1171	1.3 6.0 -	1.3 7.2 -	Top soil Weathered basement Basement Rock	H
90	1 2 3	103 71 4844	0.6 9.7 -	0.6 10.3 -	Top soil Weathered layer Basement Rock	H
102	1 2 3	39 58 479	0.9 7.5 -	0.9 8.4 -	Top soil Weathered layer Basement Rock	A
103	1 2 3	172 85 2517	0.9 22.8 -	0.9 23.7 -	Top soil Weathered layer Basement Rock	H
104	1 2 3	84 39 4334	0.9 6.3 -	0.9 7.1 -	Top soil Weathered layer Basement Rock	H

2.4 Groundwater Conditioning Factors for Potentiality Assessment

Groundwater potential assessment using remote sensing and geophysical techniques requires the identification of key controlling factors that influence groundwater occurrence and distribution, which are subsequently used as input variables in the predictive model [51]. In this study, both surface-derived and subsurface-derived parameters were considered, including aquifer resistivity, aquifer thickness, overburden thickness, transverse resistance, hydraulic conductivity, coefficient of anisotropy, aspect, and slope. These factors were selected because of their significant influence on groundwater storage, movement, recharge, and overall aquifer productivity. The hydrogeological significance of each parameter is discussed in the subsequent sections.

2.4.1 Aquifer Resistivity

The aquifer resistivity, a parameter that measures the degree of rock resistance (resistivity/conductivity) to the flow of electric current within a geological formation, indirectly measures aquifer water saturation and thus useful for providing relevant information about groundwater potential of a geological terrain. Low aquifer resistivity

inversely correlates with relatively high groundwater occurrence, with the exception of some low permeability rocks, such as clay, which may present low resistivity but poor groundwater potentiality [5].

2.4.2 Aquifer Thickness

Aquifer thickness refers to the measurement of the water-bearing formation's thickness within the subsurface. This parameter plays a crucial role in characterizing aquifers and understanding their properties. Determined from geophysical parameters, aquifer thickness provides valuable insights into the distribution of aquifer thickness across a specific area. Areas with relatively thick aquifer units are indicative of significantly high groundwater potential within that region. However, it is essential to consider exceptions such as the presence of clay material or other impermeable aquiclude materials, which can restrict groundwater movement and affect the overall aquifer's productivity and potential for groundwater extraction and use [2].

2.4.3 Overburden Thickness

Overburden thickness is the total of the materials overlying the fresh basement rocks. It has been reported by several researchers to mostly influence groundwater storage capacity in the Basement Complex terrain. Areas of thick overburden are often region of comparatively high groundwater potential than region of less overburden cover, especially where the terrain is less fractured and the overburden material is less clayey [33, 5].

2.4.4 Traverse Unit Resistance

Transverse resistance refers to the resistance of the subsurface materials to the flow of groundwater. High transverse resistance means that the subsurface materials are less permeable and have lower porosity, which can restrict the flow of groundwater [49]. This can have several implications on groundwater potential. High transverse resistance can limit the infiltration of precipitation and surface water into the subsurface, reducing the amount of water available for groundwater recharge [35]. The transverse resistance can be expressed mathematically below;

The total transverse unit resistance is defined as

$$T = \sum h_1\rho_1 + h_2\rho_2 + \cdots h_n\rho_n \quad (1)$$

2.4.5 Hydraulic Conductivity

Hydraulic conductivity is a key hydrogeological parameter that describes the ease with which water can move through porous media such as soil, sediment, or fractured rock. It reflects both the intrinsic permeability of the medium and the properties of the fluid, particularly viscosity and density [23]. High hydraulic conductivity values are associated with coarse-grained materials such as gravel and sand, which allow rapid groundwater flow, while low values are typical of fine-grained materials like clay that restrict water movement [57]. Understanding hydraulic conductivity is crucial in groundwater studies

because it controls aquifer recharge rates, influences well yields, and determines the direction and velocity of groundwater flow [3]. It is usually determined through field methods such as pumping tests, slug tests, or laboratory analysis of soil/rock samples. Accurate estimation of hydraulic conductivity is essential for groundwater resource assessment, contaminant transport modeling, and sustainable aquifer management.

2.4.6 Coefficient of Anisotropy (COA)

Coefficient of Anisotropy (COA) is a dimensionless second order geophysical parameter calculated from the transverse resistivity and longitudinal resistivity. COA shows the degree to which the subsurface lithology is inhomogeneous [20]. The heterogeneity measured by COA may results from fracturing or weathering which are necessary for secondary porosity. This secondary porosity is higher with increasing COA which ultimately indicates that, areas having higher COA will experience higher groundwater potentiality and vice versa [63].

In this study, COA is calculated using eq. 2 – eq. 5;

$$COA = \sqrt{\frac{p_{TR}}{p_{LC}}} \tag{2}$$

$$p_{TR} = \frac{TR}{H} \tag{3}$$

$$P_{LC} = \frac{H}{LC} \tag{4}$$

by substituting Eq. 3 and Eq. 4 into Eq. 2. The final formula of COA is,

$$COA = \sqrt{\frac{TR}{H} \times \frac{LC}{H}} = \frac{\sqrt{TR \times LC}}{H} \tag{5}$$

Where 'p_{TR}' is the average transverse resistivity (Ωm^2), 'P_{LC}' is the average longitudinal resistivity (Ωm^2), 'TR' is the total transverse resistance (Ωm^2), 'LC' is the total longitudinal conductance (mhos), 'H' is the thickness of the overburden materials (m), 'COA' is the coefficient of anisotropy.

2.4.7 Slope

The elevation is consequential as it reflects the ruggedness of the terrain and it is a function of the steepness of the topographic gradient. It also controls the hydraulic gradients of an area. Furthermore, elevation determines the direction of flow of surface runoff and influences meteoric recharge [16, 24]. Slope plays a vital role in the infiltration of rainfall and hence, groundwater recharge which contribute to the groundwater potentiality [47].

2.4.8 Aspect

Aspect is a topographic parameter that refers to the compass direction a slope faces, usually expressed in degrees from north (0°–360°). It plays an important role in controlling hydrological, geomorphological, and ecological processes because it influences solar radiation, evapotranspiration, soil moisture distribution, and vegetation growth [56]. In hydrogeological studies, aspect helps to understand how slope orientation affects infiltration and runoff patterns, which in turn impact groundwater recharge potential [55]. Slopes facing the sun (e.g., south-facing slopes in the northern hemisphere) often experience higher evapotranspiration, reducing water infiltration, while shaded slopes may retain more soil moisture and favor recharge [8]. Thus, aspect analysis, often derived from digital elevation models (DEMs) in GIS, provides valuable insight into land surface processes and their influence on groundwater availability and ecosystem dynamics.

2.5 Machine Learning-Based Models

Machine learning models are widely used for identifying complex patterns and making accurate predictions across diverse fields. They are commonly classified into supervised, unsupervised, and reinforcement learning approaches [58]. Supervised learning models, such as Artificial Neural Networks (ANNs) and Support Vector Machines (SVMs), learn from labeled data to predict outcomes, while unsupervised learning techniques uncover hidden patterns in unlabeled datasets [38, 29]. Reinforcement learning optimizes decision-making through reward-based interactions with the environment [54]. Recent advances have led to the development of hybrid and deep learning models that combine multiple learning techniques to improve predictive performance in complex applications [17]. Despite their growing adoption in environmental modelling and other domains, challenges related to data quality, bias, and model interpretability persist [46]. In this study, a hybrid ANN–Random Kitchen Sinks (RKS) model is employed for groundwater potential assessment.

2.5.1 Artificial Neural Network (ANN)

Artificial Neural Networks (ANNs) are brain-inspired computational models widely used for pattern recognition, classification, and prediction tasks [31]. They comprise interconnected layers of artificial neurons that process information through weighted connections and activation functions. ANN learning is commonly achieved through the backpropagation algorithm, which iteratively adjusts network weights to minimize prediction errors and improve performance [64]. Different ANN architectures, including feedforward, convolutional, and recurrent neural networks, have been successfully applied across diverse domains such as image analysis, speech recognition, and time-series forecasting [26]. Although ANNs offer strong predictive capabilities, their performance may be constrained by issues such as overfitting, high computational requirements, and dependence on large datasets [52]. Nevertheless, they remain one of

the most effective machine learning techniques for modelling complex nonlinear relationships [10].

The fundamental equation of an Artificial Neural Network (ANN) is based on the weighted sum of inputs, followed by an activation function. The mathematical representation for a single neuron is:

$$y = f(\sum_{i=1}^{n} wixi + b) \quad (6)$$

Where: y = Output of the neuron; xi = Inputs (features); wi = Weights associated with each input; b = Bias term; f (·) = Activation function (e.g., ReLU, Sigmoid, Tanh); n = Number of input features

2.5.2 Random Kitchen Sinks (RKS)

Rahimi and Recht [43] developed the Random Kitchen Sinks (RKS) technique, which uses random feature mappings to effectively approximate nonlinear kernel functions. Conventional kernel techniques, such as the Radial Basis Function (RBF) kernel, can have a high computational complexity, particularly when dealing with big datasets. By converting input data into a randomized feature space, RKS solves this problem and makes it possible for linear models to estimate intricate non-linear functions at a lower computing cost [43]. The transformation is defined as:

$$\phi(x) = cos(Wx + b) \quad (7)$$

Where, W is a random weight matrix sampled from a Gaussian distribution; b is a bias term, and
cos (·) serves as a nonlinear mapping function.

2.6 ANN-RKS Model Development

Artificial Neural Network (ANN) and Radial Basis Function Random Kitchen Sinks–Ridge Regression (RKS–Ridge) models were employed to investigate the nonlinear relationship between geophysical and hydrogeological parameters and groundwater yield. Eight predictor variables—aspect, slope, aquifer thickness, coefficient of anisotropy (COA), hydraulic conductivity, overburden thickness, resistivity of the weathered layer, and traverse resistance—were used, while groundwater yield served as the target variable and the VES identifier was excluded from the predictors. All data preprocessing, model development, hyperparameter tuning, cross-validation, and performance evaluation were conducted using Python programming software. The analysis utilised pandas and NumPy for data manipulation, TensorFlow/Keras for ANN development, and scikit-learn for data preprocessing, random-feature generation, Ridge regression, cross-validation, and performance evaluation. Data preprocessing involved removing whitespace from column names, replacing infinite values with missing values, removing entirely empty columns, excluding non-numeric predictors, and imputing missing values using the mean for ANN and the median for RKS–Ridge. Both models employed a logarithmic target transformation, ($y' = \ln(1+y)$), with predictions subsequently converted to the original scale using ($\hat{y} = e^{\hat{y}} - 1$), and negative predictions were set to zero. The ANN was implemented as a feed-forward multilayer

perceptron with two hidden layers containing 16 and 8 neurons, respectively, using ReLU activation, a linear output layer, the Adam optimiser with a learning rate of 0.001, mean squared error loss, gradient clipping at 1.0, a maximum of 200 epochs, a batch size of 8, and early stopping with a patience of 20 epochs. MinMaxScaler was used to scale predictors and the transformed target, while a random seed of 42 supported reproducibility. The RKS–Ridge model used RobustScaler to scale predictors, RBFSampler to approximate the radial basis function kernel through random Fourier features, and Ridge regression with L2 regularisation. Its hyperparameters were optimised over six equally spaced (γ) values between 0.01 and 0.30, random-feature dimensions of 200, 400, 600, and 800, and regularisation parameters (α) of 0.01, 0.1, 1, and 5. Model performance was intended to be assessed using shuffled 10-fold cross-validation with a random state of 42 and evaluated using mean absolute error (MAE), mean squared error (MSE), root mean squared error (RMSE), and the coefficient of determination (R^2), calculated on the original groundwater-yield scale.

2.7 Validation and Performance Evaluation of Groundwater Potential Models

The reliability of the groundwater potential maps (GPMs) generated using the Artificial Neural Network (ANN) and ANN–Random Kitchen Sinks (ANN-RKS) models were assessed through validation against field data obtained from existing hand-dug wells within the study area. Validation involved both qualitative and quantitative spatial attribute correlation analyses, comparing predicted groundwater potential zones with well water column measurements [27]. Water column levels were determined as the difference between total well depth and static water level (table 2), providing an indicator of groundwater occurrence and storage capacity [5, 7]. The degree of agreement between groundwater potential classes and observed well conditions was used to evaluate the predictive reliability of the generated maps. Model performance was further evaluated using Root Mean Square Error (RMSE), Mean Absolute Error (MAE), Mean Squared Error (MSE), and the Coefficient of Determination (R^2). These metrics were used to assess prediction accuracy, error magnitude, model generalization, and goodness-of-fit [36]. The ANN-RKS model was expected to outperform the conventional ANN model by producing lower RMSE, MAE, and MSE values and a higher R^2 value, indicating improved predictive capability and robustness for groundwater potential assessment.

Table 2: Hand-dug Well Parameters in the Study Area

Location	Easting (mE)	Northing (mN)	Well Depth (m)	Elevation (m)	Static water level (m)	Saturated thickness of the Aquifer (m)
W1	737243	804308	9.5	376	7.2	2.3
W2	737105	804919	12	364	8.3	3.7
W3	736386	805774	14.2	387	11.5	2.7
W4	736200	805060	7.8	359	6.6	1.2
W5	736712	803964	11.5	380	9.4	2.1
W6	736843	803956	13.6	373	11.8	1.8
W7	737062	804605	16.5	355	10.2	6.3
W8	736525	804408	8.9	378	4.9	4
W9	736988	803949	11.7	362	5.9	5.8
W10	735559	805485	14.8	370	12.1	2.7
W11	737031	803588	9.3	381	4.5	4.8
W12	737622	803706	12.6	375	10.6	2
W13	736284	804199	17.2	357	14.5	2.7
W14	735472	805836	9.8	385	5.8	4
W15	737904	804916	11.9	360	6.7	5.2
W16	735828	806047	8.5	389	6.8	1.7
W17	736535	804656	12.8	377	8	4.8
W18	735993	805826	11.1	369	6.2	4.9
W19	736019	805624	9.6	384	7.4	2.2
W20	736504	805193	12.1	382	8	4.1

W21	736716	805076	10.4	379	3.9	6.5
W22	736456	804993	13	353	11.6	1.4
W23	736799	803787	14.7	390	10.5	4.2
W24	736715	805078	8.2	371	4.7	3.5
W25	737102	804919	11.6	358	9.6	2
W26	737056	805076	13.4	368	11.1	2.3
W29	736835	805162	9.1	349	8.2	0.9
W28	736185	805468	14.1	334	8.2	5.9
W29	736778	804109	17.5	370	15.3	2.2
W30	737794	804157	12.2	349	6	6.2
W31	737533	804100	15	350	13	2
W32	737317	804928	14	376	7	7
W33	736755	805114	12	345	8	4
W34	736467	804968	20	335	9	11
W35	736473	804941	14	329	12	2
W36	736476	804915	11	332	10	1
W37	736526	804820	16	336	12	4
W38	736534	804777	14	335	13.5	0.5
W39	736762	804772	16	360	12	4
W40	736759	804555	15	359	14	1

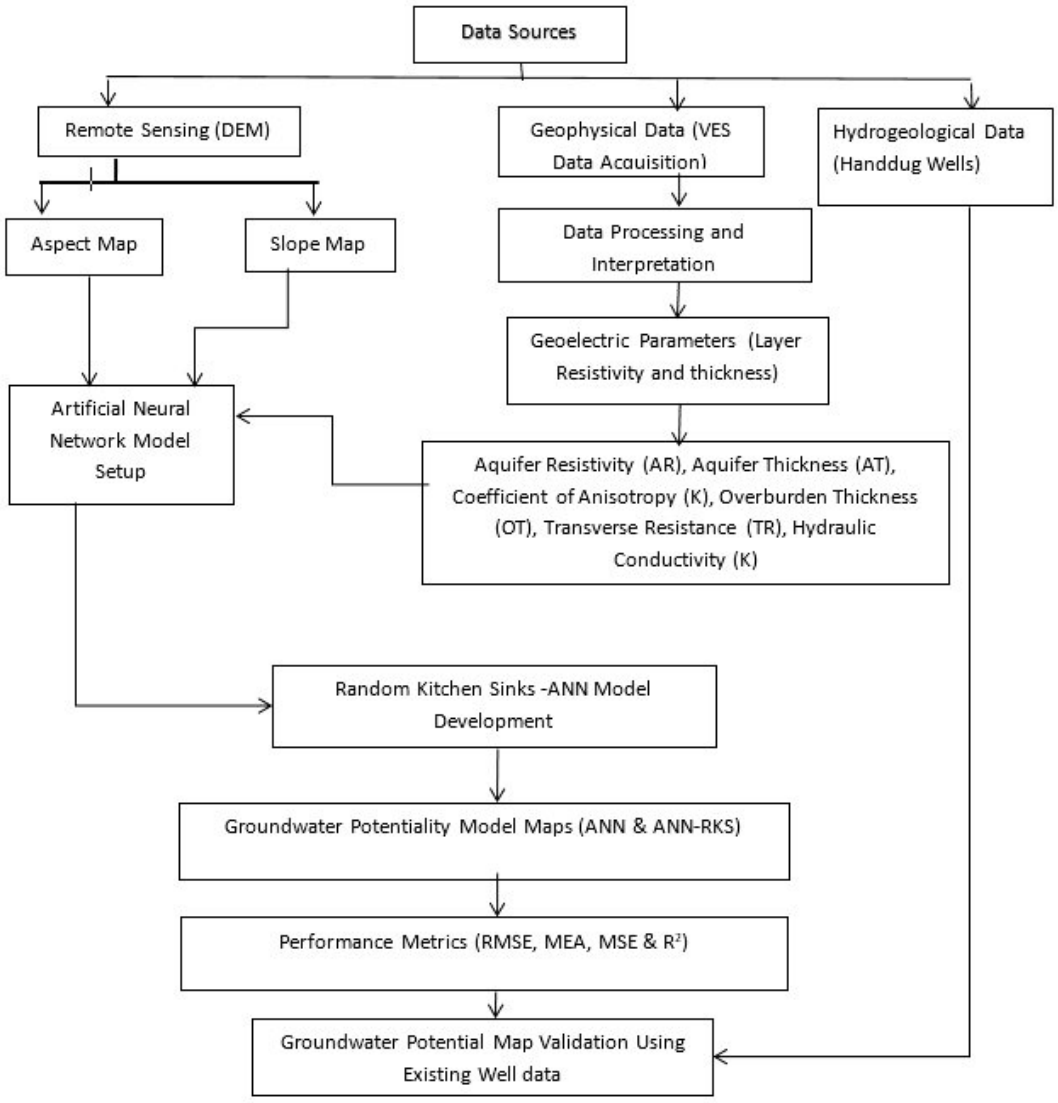


Fig. 6: Methodology Flow Chart.

3. Discussion of Results

3.1 Remote Sensing Results

3.1.1 Slope Degree

The slope map (Fig. 7) classified the study area into four categories: Very Low (0°–2.71°), Low (2.72°–4.74°), Moderate (4.75°–7.44°), and High (7.45°–14.38°). The Very Low and Low slope classes cover approximately 74% of the study area, indicating predominantly gentle terrain conditions. These low-gradient areas favour water infiltration and groundwater recharge due to reduced surface runoff. Conversely, the Moderate and High slope classes, which occupy about 26% of the area, are associated with increased runoff and reduced infiltration, resulting in comparatively lower groundwater recharge potential.

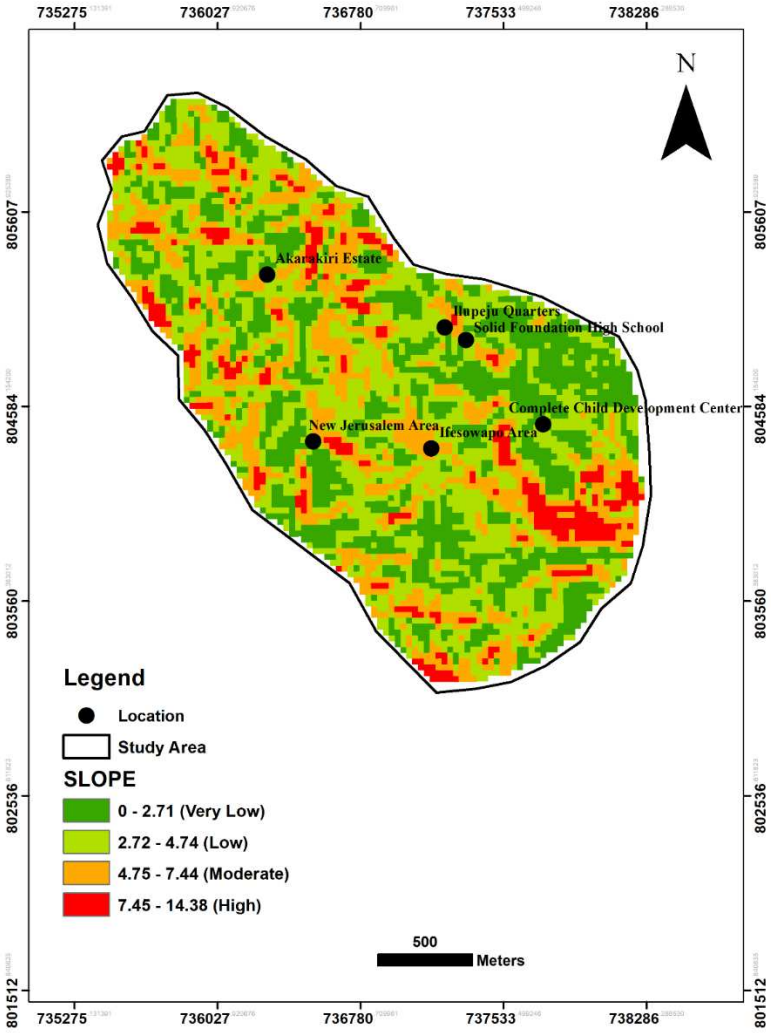


Fig. 7: Slope Degree Map of the Study Area

3.1.2 Aspect Degree

The aspect map (Fig. 8) classified the study area into four categories: Very Low (1°–82.17°), Low (82.18°–172.38°), Moderate (172.39°–264.01°), and High (264.02°–358.45°), covering approximately 22%, 18%, 35%, and 25% of the area, respectively. The Very Low and Low aspect zones are associated with lower runoff, longer water residence time, and enhanced infiltration, making them more favourable for groundwater recharge. In contrast, the Moderate and High aspect zones, which dominate the study area, promote organized surface flow, increased runoff, and reduced infiltration, resulting in lower groundwater recharge potential.

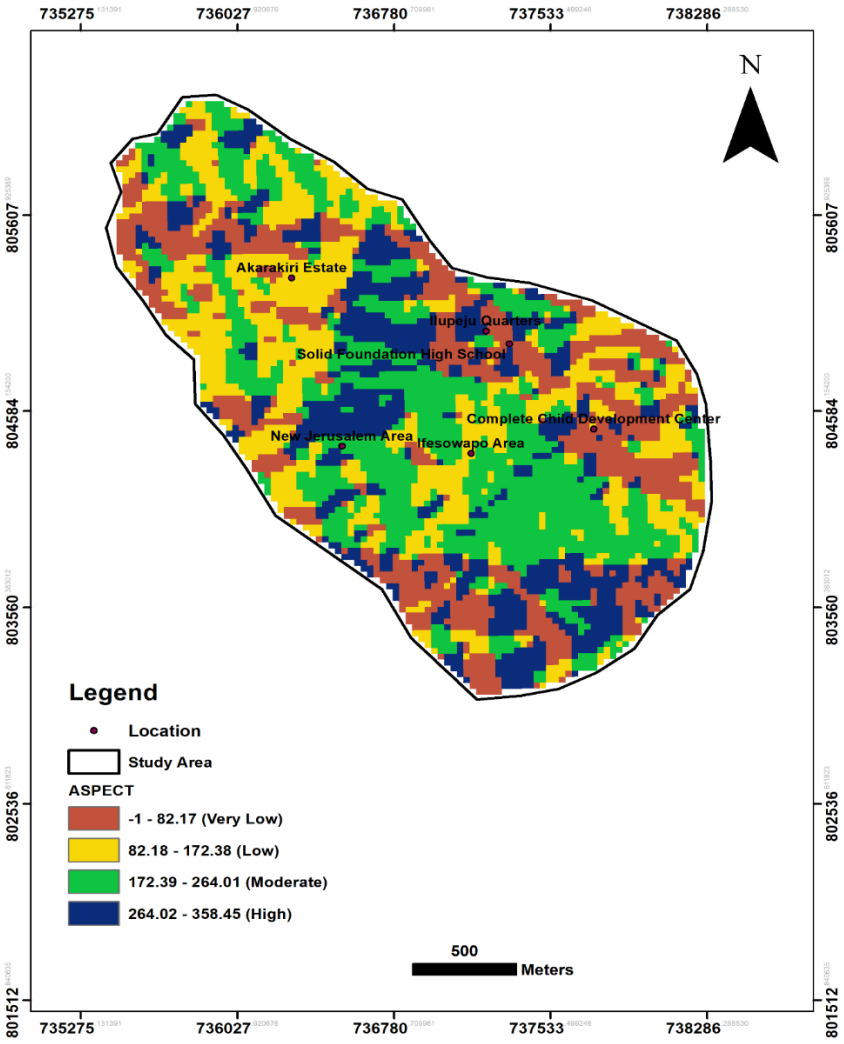


Fig. 8: Aspect Degree Map of the Study Area

3.2 Electrical Resistivity Results

3.2.1 Weathered Layer Resistivity Map

The resistivity map (Fig. 9) shows values ranging from 7 to 1,497 Ωm and classifies the study area into four zones: Very Low (7–124 Ωm), Low (125–264 Ωm), Moderate (265–568 Ωm), and High (569–1,497 Ωm). Very Low resistivity zones are associated with clay-rich and water-saturated materials that exhibit low hydraulic conductivity and limited groundwater potential. Low resistivity zones represent weathered formations with moderate porosity and permeability, making them favourable for groundwater occurrence. Moderate resistivity zones, corresponding to granular weathered materials and fractured basement rocks, exhibit the highest groundwater potential due to enhanced permeability and effective porosity. In contrast, High resistivity zones are indicative of fresh basement rocks with limited pore space and generally poor groundwater storage capacity.

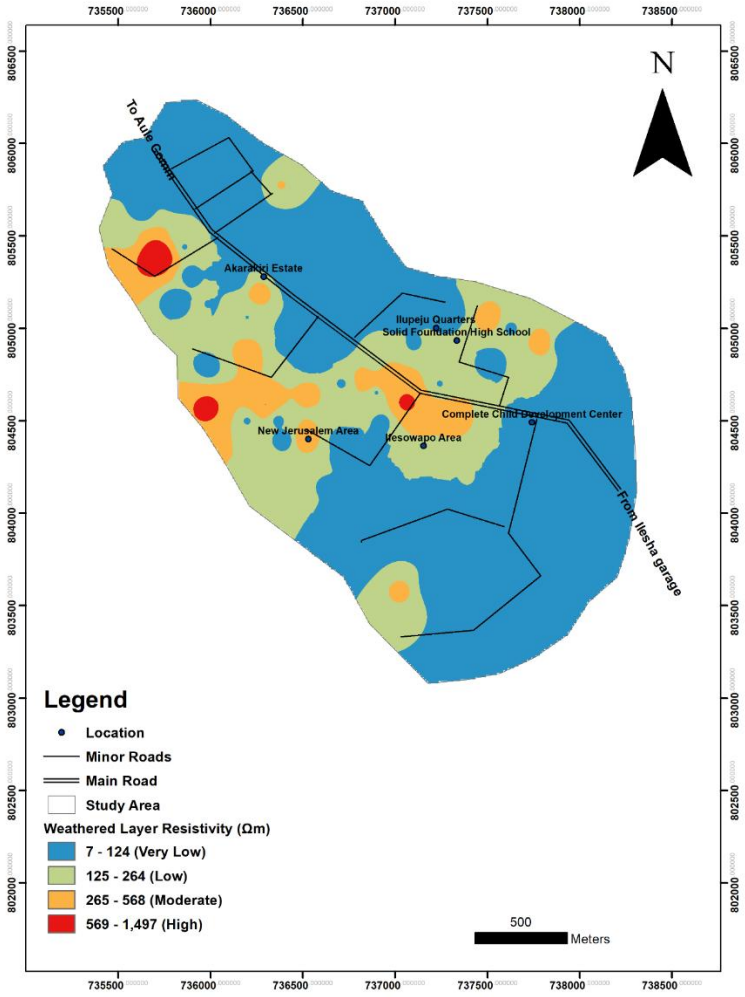


Fig. 9: Weathered layer Resistivity Map of the Study Area

3.2.2 Overburden Thickness (OT)

The overburden thickness map (Fig. 10) shows values ranging from 1.9 m to 73.8 m and classifies the study area into four categories: Very Low (1.9–7.8 m), Low (7.9–14.3 m), Moderate (14.4–30.7 m), and High (30.8–73.8 m). Areas with Very Low and Low overburden thickness are characterized by shallow weathering and limited groundwater storage capacity, making groundwater occurrence largely dependent on fractures within the basement rock. Moderate thickness zones indicate well-developed weathered profiles that support improved groundwater infiltration, storage, and transmission. High thickness zones, although less extensive, possess substantial storage capacity and are the most favourable for groundwater development. Overall, groundwater potential increases with overburden thickness, with the Moderate and High thickness zones (≥14.4 m) representing the most promising areas for sustainable groundwater exploitation.

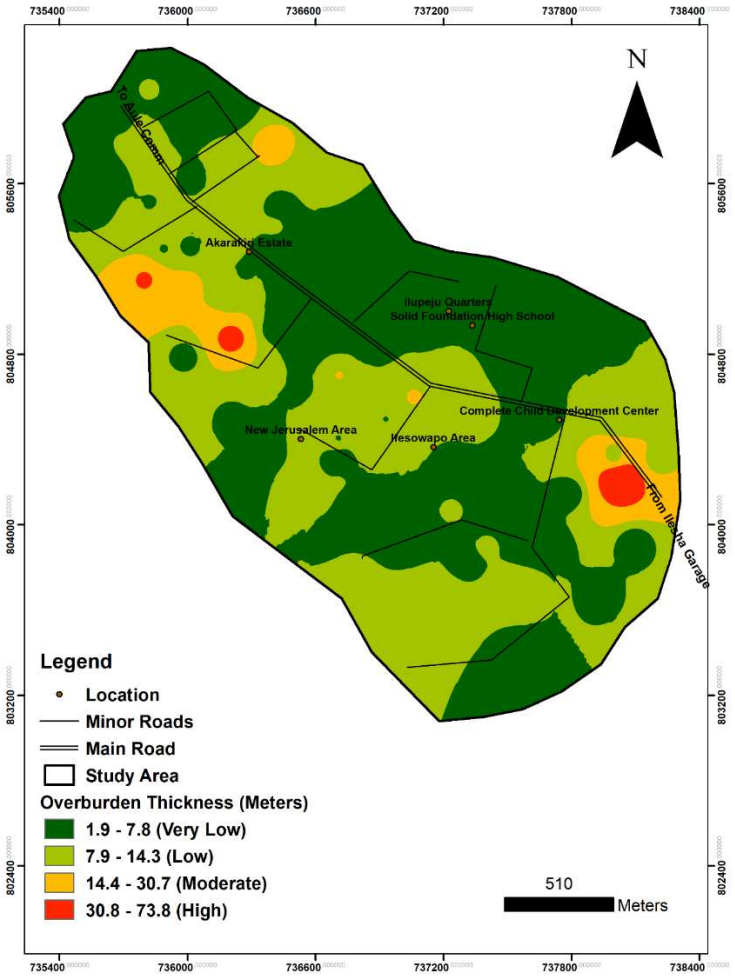


Fig. 10: Overburden Thickness Map of the Study Area

3.2.3 Aquifer Thickness (AT)

The aquifer thickness map (Fig. 11) reveals considerable spatial variation, with values ranging from 0.3 m to 55.9 m and classified into Very Low (0.3–7.3 m), Low (7.4–13.0 m), Moderate (13.1–24.7 m), and High (24.8–55.9 m) categories. Very Low and Low thickness zones dominate much of the study area and are characterized by limited groundwater storage, low transmissivity, and reduced borehole yield potential. In contrast, Moderate thickness zones exhibit improved storage capacity and transmissivity, making them favourable for groundwater development. High thickness zones, although limited in extent, possess the greatest groundwater potential due to their substantial saturated thickness, enhanced transmissivity, and capacity to sustain long-term abstraction.

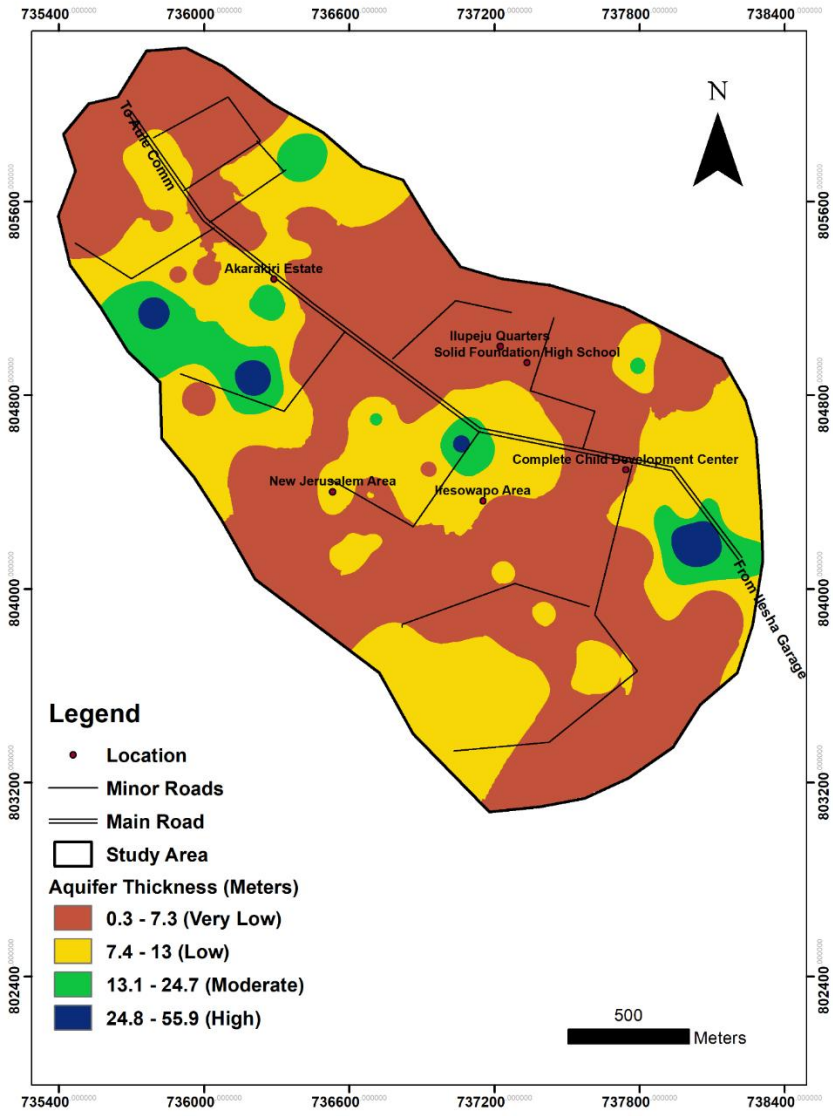


Fig. 11: Aquifer Thickness Map of the Study Area

3.2.4 Hydraulic Conductivity

The hydraulic conductivity map (Fig. 12) shows values ranging from 0 to 0.052 m/day and classifies the study area into Very Low (0–0.019 m/day), Low (0.02–0.029 m/day), Moderate (0.03–0.037 m/day), and High (0.038–0.052 m/day) categories. Very Low and Low hydraulic conductivity zones are associated with low-permeability materials, restricted groundwater flow, and poor borehole yield potential. In contrast, Moderate conductivity zones indicate appreciable permeability and improved groundwater transmission, making them favourable for groundwater development. High conductivity zones, though less extensive, represent highly permeable formations with efficient groundwater flow, high transmissivity, and strong recharge potential.

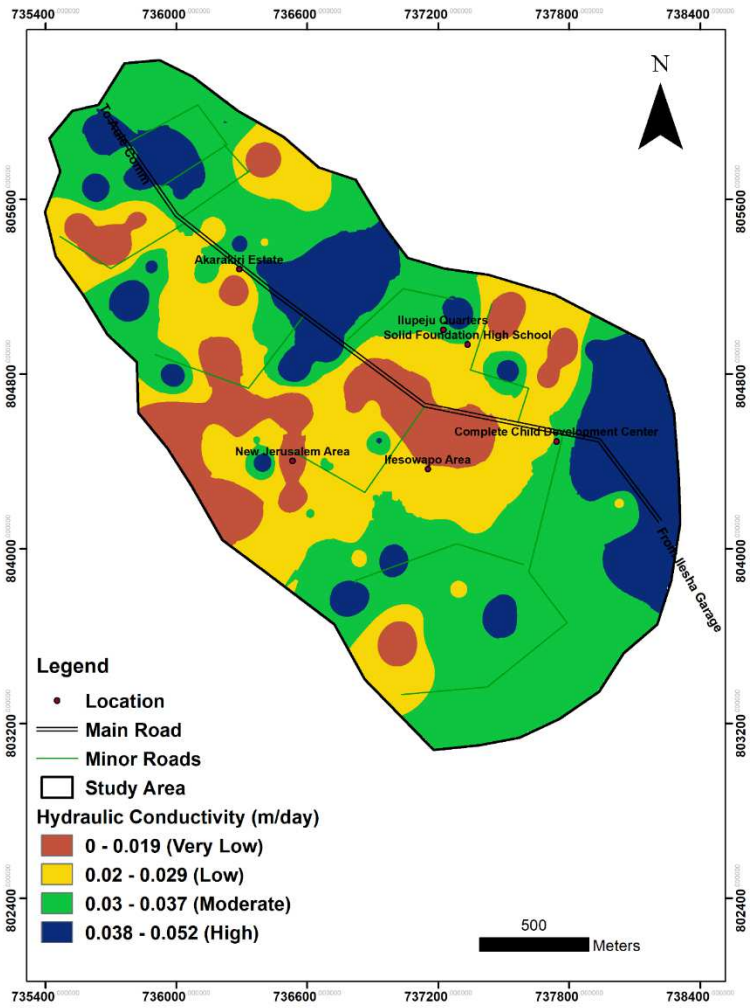


Fig. 12: Hydraulic Conductivity Map of the Study Area

3.2.5 Transverse Resistance

The transverse resistance map (Fig. 13) classifies the study area into Very Low (72–1,582 Ωm), Low (1,583–4,299 Ωm), Moderate (4,300–10,136 Ωm), and High (10,137–25,735 Ωm) categories. Very Low transverse resistance zones dominate the area and are associated with thin overburden or clay-rich materials, resulting in low transmissivity, limited groundwater storage, and poor aquifer performance. Low resistance zones indicate moderate groundwater potential, with slight improvements in aquifer thickness and permeability. Moderate transverse resistance zones reflect favourable combinations of aquifer thickness and resistivity, supporting enhanced groundwater storage and transmissivity. High transverse resistance zones, although limited in extent, represent the most favourable conditions for groundwater development due to their thick, permeable, and well-protected aquifer systems.

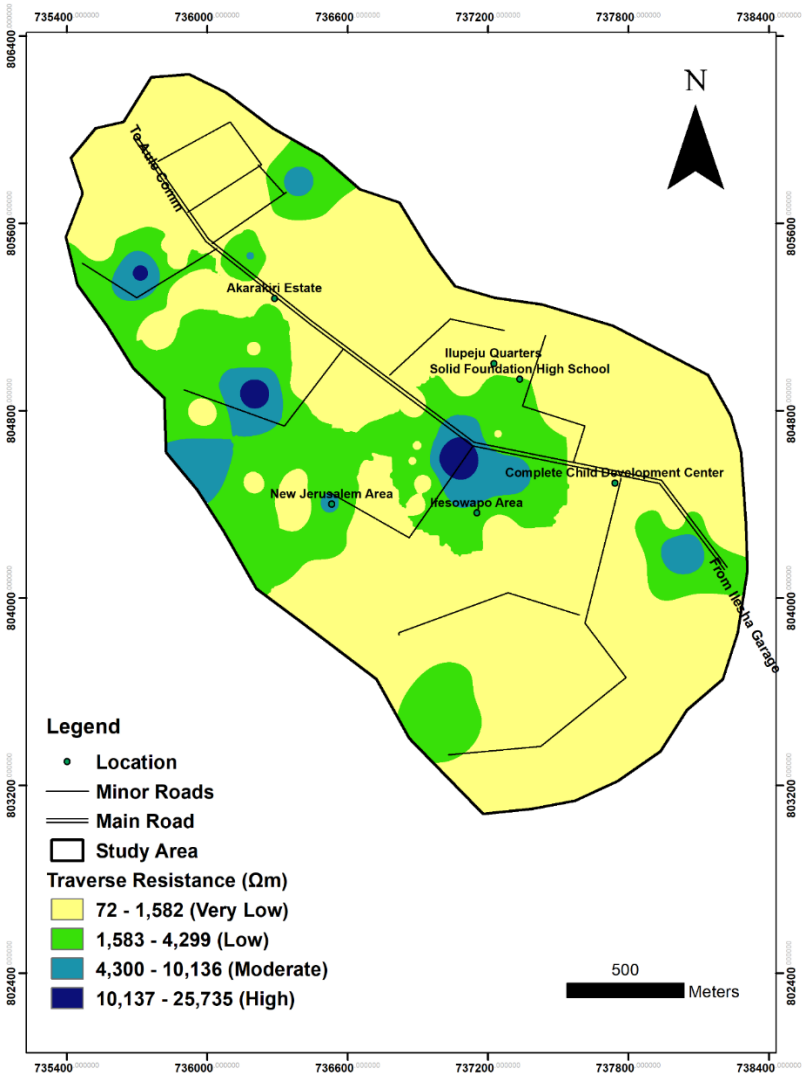


Fig. 13: Traverse Resistance Map of the Study Area

3.2.6 Coefficient of Anisotropy (λ)

The coefficient of anisotropy map (Fig. 14) shows values ranging from 1.000 to 2.492 and classifies the study area into Very Low (1.000–1.117), Low (1.118–1.275), Moderate (1.276–1.585), and High (1.586–2.492) categories. Very Low and Low anisotropy zones dominate the area and are characterized by relatively uniform subsurface conditions, limited fracturing, and restricted groundwater movement, resulting in low groundwater potential. Moderate anisotropy zones indicate increased subsurface heterogeneity, weathering, and fracturing, which enhance secondary porosity and groundwater transmission. High anisotropy zones, although limited in extent, are associated with intensely fractured formations and well-connected permeability pathways, making them the most favourable for groundwater accumulation and exploitation.

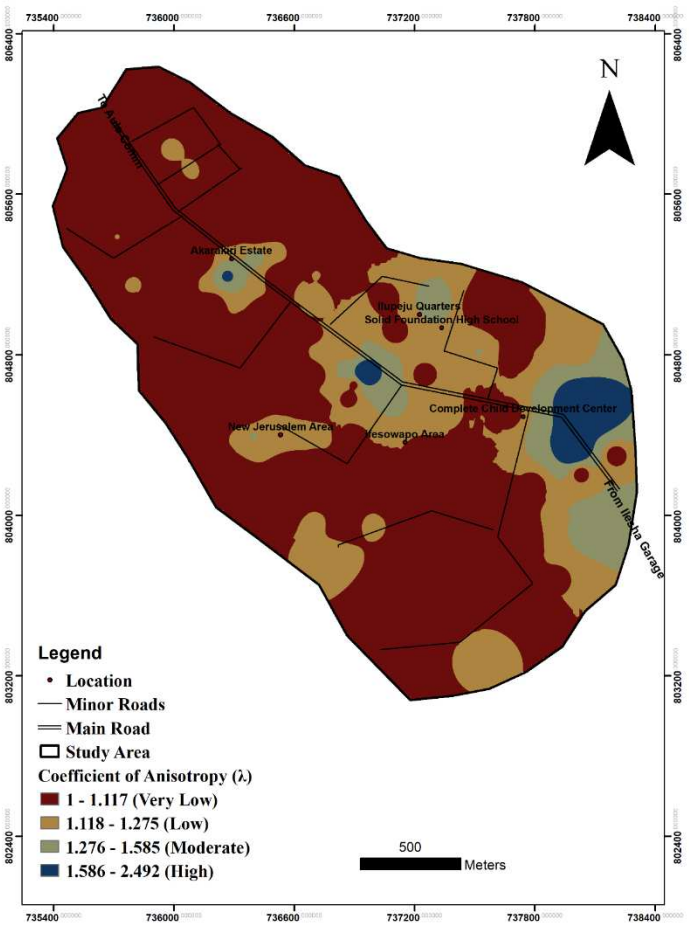


Fig. 14: Coefficient of Anisotropy (λ) Map of the Study Area

4. **Groundwater Potential Model Map of the Study Area**

Comparative analysis of the Artificial Neural Network (ANN) shown in Fig. 15 and ANN–Random Kitchen Sinks (ANN-RKS) (Fig. 16) groundwater potential models revealed that the ANN-RKS model provided superior predictive accuracy and more detailed spatial delineation of groundwater potential zones. Both models identified areas of very low, low, moderate, and high groundwater potential; however, the ANN-RKS model produced clearer boundaries and more realistic transitions between hydrogeological units.

The groundwater potential maps indicate that approximately 60–65% of the study area falls within the very low to low potential classes, reflecting generally unfavourable conditions characterized by limited aquifer thickness, low permeability, and weak structural development. In contrast, about 35–40% of the area exhibits moderate to high groundwater potential, occurring as localized zones associated with favourable hydrogeological conditions. These zones are characterized by enhanced porosity, permeability, transmissivity, and aquifer storage capacity, making them suitable targets for groundwater development and sustainable abstraction.

The improved performance of the ANN-RKS model is attributed to its ability to capture complex nonlinear relationships between groundwater occurrence and controlling hydrogeophysical parameters. High-potential zones identified by the model correspond closely with areas exhibiting favourable resistivity characteristics, moderate to high

aquifer and overburden thicknesses, enhanced hydraulic conductivity, and favourable anisotropy conditions. The model also demonstrates strong agreement with transverse resistance distributions, indicating areas with improved groundwater storage and transmission properties. Overall, the ANN-RKS model provided a more reliable representation of groundwater potential across the study area and was therefore considered the preferred model for groundwater exploration and resource assessment.

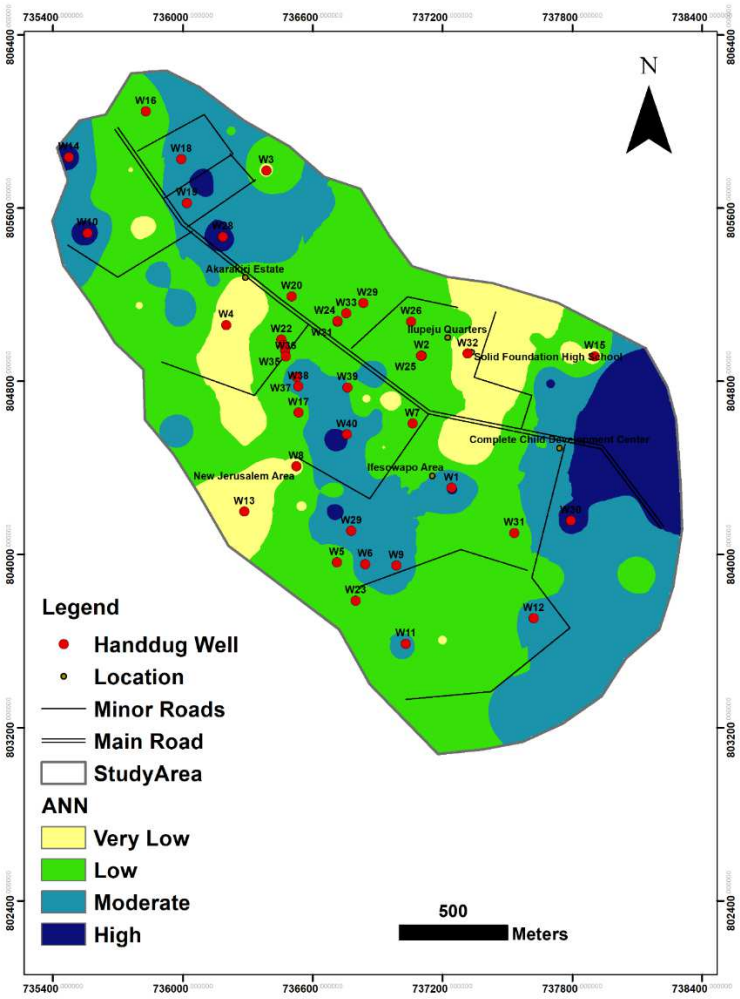


Fig. 15: ANN Groundwater Potential Map of the Study Area

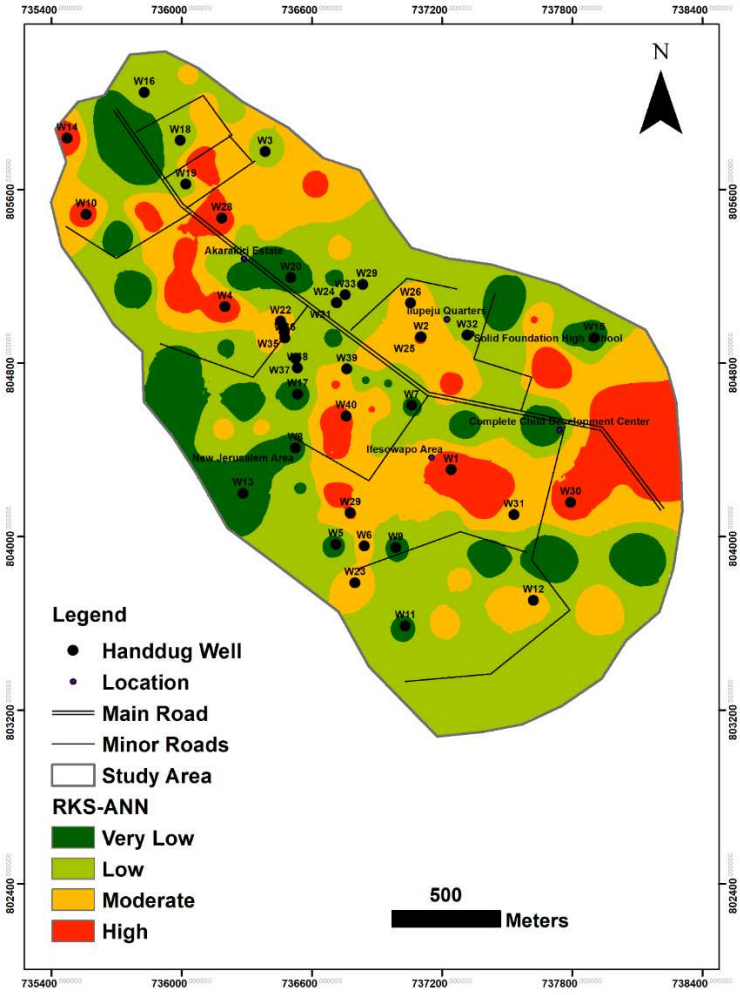


Fig. 16: ANN-RKS Groundwater Potential Map of the Study Area

4.2 Validation of the Groundwater Potential Model Map

Validation of the groundwater potential model was performed using saturated thickness measurements from hand-dug wells and borehole yield data. The ANN-RKS model exhibited stronger predictive performance and better agreement with observed field data than the conventional ANN model. Spatial comparison revealed that many wells located within moderate- to high-potential zones corresponded to productive groundwater locations, particularly in the northwestern and southeastern parts of the study area. However, variations in well performance within similar potential classes highlight the heterogeneous nature of Basement Complex aquifers, where groundwater occurrence is strongly influenced by local variations in weathering, lithology, and fracture development. Overall, approximately 60–70% of the wells were located within moderate- to high-potential zones, yielding a validation accuracy of about 64%. The improved performance of the ANN-RKS model demonstrates its ability to capture complex nonlinear relationships between hydrogeophysical parameters and groundwater occurrence. Consequently, the ANN-RKS framework proved effective for groundwater potential assessment and

borehole siting, although detailed site-specific investigations remain necessary to optimize groundwater development.

4.3 Performance Evaluation of ANN and ANN-RKS Models

The performance of the ANN and ANN-RKS models was evaluated using MAE, MSE, RMSE, and R^2 metrics (Table 3). The ANN model achieved MAE, MSE, RMSE, and R^2 values of 0.082, 0.012, 0.109, and 0.81, respectively, indicating good predictive capability but limited representation of complex nonlinear groundwater relationships. The ANN-RKS model showed improved performance, with lower error values (MAE = 0.056, MSE = 0.006, RMSE = 0.078) and a higher coefficient of determination (R^2 = 0.91). These results demonstrate that the incorporation of Random Kitchen Sinks enhanced the model's ability to capture nonlinear hydrogeophysical interactions, resulting in more accurate groundwater potential predictions, reduced prediction bias, and stronger agreement with field observations.

Table 3: Performance Metrics between the ANN and ANN-RKS Models

Performance Metric	**ANN**	**ANN-RKS**
Mean Absolute Error (MAE)	0.082	0.056
Mean Squared Error (MSE)	0.012	0.006
Root Mean Squared Error (RMSE)	0.109	0.078
Coefficient of Determination (R^2)	80.1%	91.0%

The comparative analysis of performance metrics clearly demonstrates that the ANN-RKS model outperformed the conventional ANN, offering higher accuracy, improved reliability, and greater robustness during field validation. Consequently, the ANN-RKS model represents a more effective decision-support tool for groundwater exploration, particularly in geologically complex terrains such as the study area.

5. Conclusion

This study integrated hydrogeological, geophysical, GIS, and machine learning techniques to evaluate groundwater potential in Aule Community, Akure, Southwestern Nigeria. A total of 105 Vertical Electrical Soundings (VES), hand-dug well measurements, and terrain-derived factors such as slope and aspect were utilized to characterize subsurface conditions and develop groundwater potential models.

VES interpretation identified five geoelectric curve types, with the H-type curve predominating (69.5%), indicating a typical Basement Complex environment characterized by weathered and fractured basement aquifers. The results revealed significant spatial variability in aquifer properties, with groundwater occurrence largely controlled by weathered layer thickness, fracturing, permeability, and lithological composition. Although the weathered/fractured basement constitutes the principal aquifer

unit, its generally thin and clay-rich nature imposes constraints on groundwater storage and productivity.

The ANN and ANN-RKS models successfully predicted groundwater potential using hydrogeophysical and terrain parameters. However, the ANN-RKS model consistently outperformed the conventional ANN model, achieving lower prediction errors and a higher coefficient of determination. The incorporation of Random Kitchen Sinks enhanced the model's ability to capture complex nonlinear relationships among groundwater conditioning factors, resulting in improved predictive accuracy and spatial delineation of groundwater potential zones.

Validation with hand-dug well data confirmed the reliability of the generated groundwater potential maps, with the ANN-RKS model showing stronger agreement with observed groundwater conditions and better representation of hydrogeological variability across the study area. The results indicate that groundwater potential is generally low to moderate across much of the area, with localized zones of high potential associated with favorable aquifer thickness, hydraulic conductivity, weathering intensity, and fracture development. Overall, the study demonstrates that the integration of geophysical data and advanced machine learning techniques provides an effective framework for groundwater potential assessment in Basement Complex terrains. The ANN-RKS model proved to be a robust and reliable tool for groundwater exploration, borehole siting, and sustainable groundwater resource management, offering improved predictive performance over the conventional ANN approach.

Declarations

Author contribution statement

T. D. Akande, O. J. Akintorinwa: Conceived and designed the research methodology; Performed the field data acquisition; Analyzed and interpreted the data; developed the models wrote the paper. All authors have read, edited, and agreed to publish the manuscript.

Data availability

The data supporting the findings of this study are available from the corresponding author, Akande, Timilehin Damilare, upon reasonable request. Requests for access to the raw hydrogeophysical data, hand-dug well records, and derived datasets should be directed to akandedamilare.t@gmail.com

Funding statement

This research did not receive any specific grant from funding agencies in the public, commercial, or not-for-profit sectors.

Competing interest statement

The authors declare no conflict of interest.

Ethical approval

The study complied with all ethical guidelines.

Consent to Participate
Not applicable.

Consent to Publish
Not applicable. The manuscript does not contain personal identifiable data or contents of any individual

References

1. Aderemi, B. A., Olwal, T. O., Ndambuki, J. M., & Rwanga, S. S. (2021). A review of groundwater management models with a focus on IoT-based systems. *Sustainability*, *14*(1), 148.
2. Adiat, K. A. N., Ajayi, O. F., Akinlalu, A. A., and Tijani, I. B. (2020). Prediction of groundwater level in basement complex terrain using artificial neural network: a case of Ijebu-Jesa, southwestern Nigeria. Applied Water Science, 10, Pp. 1-14.
3. Akhtar, N., Syakir, M. I., Anees, M. T., Qadir, A., & Yusuff, M. S. (2020). Characteristics and assessment of groundwater. In M. I. Syakir, A. Qadir, & M. S. Yusuff (Eds.), *Groundwater management and resources*. IntechOpen. https://doi.org/10.5772/intechopen.92014
4. Akingboye, A. S. (2024). Unraveling subsurface crustal dynamics: exploring electrical and seismic refraction methods from theories to existing and machine learning-based emerging prospects. *arXiv preprint arXiv:2404.00813*.
5. Akinlalu, A. A., Adegbuyiro, A., Adiat, K. A. N., Akeredolu, B. E., and Lateef, W. Y. (2017). Application of multi-criteria decision analysis in prediction of groundwater resources potential: a case of Oke-Ana, Ilesa Area Southwestern, Nigeria. NRIAG Journal of Astronomy and Geophysics, 6(1), Pp.184-200.
6. Bamal, A., Uddin, M. G., & Olbert, A. I. (2024). Harnessing machine learning for assessing climate change influences on groundwater resources: a comprehensive review. *Heliyon*, *10*(17).
7. Bayode, S., Mogaji, K. A., and Egbeyemi, O. (2024). Modeling of geophysical derived parameters for groundwater potential zonation using GIS-based multi-criteria conceptual model. *Applied Water Science*, 14(2), Pp.19.
8. Bilir, T. E., Fung, I., & Dawson, T. E. (2021). Slope-aspect induced climate differences influence how water is exchanged between the land and atmosphere. *Journal of Geophysical Research: Biogeosciences, 126*(5), e2020JG006027. https://doi.org/10.1029/2020JG006027
9. Davamani, V., John, J. E., Poornachandhra, C., Gopalakrishnan, B., Arulmani, S., Parameswari, E., & Naidu, R. (2024). A critical review of climate change impacts on groundwater resources: a focus on the current status, future possibilities, and role of simulation models. *Atmosphere*, *15*(1), 122.
10. Devarapu, K. (2021). Advancing Deep Neural Networks: Optimization Techniques for Large-Scale Data Processing. *NEXG AI Review of America*, *2*(1), 47-61.
11. Egbueri, J. C., & Agbasi, J. C. (2022). Data-driven soft computing modeling of groundwater quality parameters in southeast Nigeria: comparing the performances of different algorithms. *Environmental Science and Pollution Research*, *29*(25), 38346-38373.

12. Etuk, M., Re, V., Viaroli, S., Raco, B., & Igwe, O. (2025). Assessing groundwater quality and solute sources in highly anthropized areas. The case of Abuja Federal Capital Territory, Nigeria. *Groundwater for Sustainable Development*, *29*, 101425.
13. Falowo, O. O., Oluwasegunfunmi, V., Akindureni, Y., Olabisi, W., & Aliu, A. (2019). Groundwater physicochemical characteristics and water quality index determination from selected water wells in Akure, Ondo State, Nigeria. American Journal of Water Resources, 7(2), 76–88. https://doi.org/10.12691/ajwr-7-2-5.
14. Gan, B. Y., Leykam, D., & Angelakis, D. G. (2022). Fock state-enhanced expressivity of quantum machine learning models. *EPJ Quantum Technology*, *9*(1), 16.
15. Ibrahim, A., Toyin, A. and Sanni, Z. J., (2015). Geological characteristics and petrographic analysis of rocks of Ado-Awaiye and its Environs, Southwestern Nigeria. *International Journal of Applied Science and Mathematical Theory*, *1*(8), Pp.28-47.
16. Jha, M. K., Chowdary, V. M., and Chowdhury, A. (2010). Groundwater assessment in Salboni Block, West Bengal (India) using remote sensing, geographical information system and multi-criteria decision analysis techniques. *Hydrogeology journal,* 18(7), Pp.1713-1728.
17. Jia, J., Liang, W., & Liang, Y. (2023). A review of hybrid and ensemble in deep learning for natural language processing. *arXiv preprint arXiv:2312.05589*.
18. Kalu, I., Ndehedehe, C. E., Okwuashi, O., Eyoh, A. E., & Ferreira, V. G. (2022). A new modelling framework to assess changes in groundwater level. *Journal of Hydrology: Regional Studies*, *43*, 101185.
19. Keay, S., Lister, G. and Buick, I., (2001). The timing of partial melting, Barrovian metamorphism and granite intrusion in the Naxos metamorphic core complex, Cyclades, Aegean Sea, Greece. *Tectonophysics*, *342*(3-4), Pp.275-312.
20. Knochenmus, L. A., and Robinson, J. L. (1996). Descriptions of anisotropy and heterogeneity and their effect on ground-water flow and areas of contribution to public supply wells in a karst carbonate aquifer system, US Government Printing Office.(Vol. 2475).
21. Lachassagne, P., Dewandel, B., & Wyns, R. (2021). Hydrogeology of weathered crystalline/hard-rock aquifers—guidelines for the operational survey and management of their groundwater resources. *Hydrogeology Journal*, *29*(8), 2561-2594.
22. Lange, H., & Sippel, S. (2020). Machine learning applications in hydrology. *Forest-water interactions*, 233-257.
23. Liu, H. H. (2022). The large-scale hydraulic conductivity for gravitational fingering flow in unsaturated homogenous porous media: A review and further discussion. *Water, 14*(22), 3660. https://doi.org/10.3390/w14223660
24. Magesh, N. S., Chandrasekar, N., and Soundranayagam, J. P. (2012). Delineation of groundwater potential zones in Theni district, Tamil Nadu, using remote sensing, GIS and MIF techniques. *Geoscience frontiers*, 3(2), Pp.189-196.
25. Mensah, V., Boateng, C. D., Gidigasu, S. S., Wemegah, D. D., Aryee, J. N., Osei, M. A., ... & Afful, S. K. (2024). Groundwater Exploration Methods in West Africa: A Review.

26. Mienye, I. D., Swart, T. G., & Obaido, G. (2024). Recurrent neural networks: A comprehensive review of architectures, variants, and applications. *Information*, *15*(9), 517.
27. Mogaji, K. A. and Omobude, O. B., (2017). Modeling of geoelectric parameters for assessing groundwater potentiality in a multifaceted geologic terrain, Ipinsa Southwest, Nigeria–A GIS-based GODT approach. NRIAG Journal of Astronomy and Geophysics, 6(2), Pp.434-451.
28. Mukherjee, A., Scanlon, B. R., Aureli, A., Langan, S., Guo, H., & McKenzie, A. (2021). Global groundwater: from scarcity to security through sustainability and solutions. In *Global groundwater* (pp. 3-20). Elsevier.
29. Neuer, M. J. (2024). Unsupervised learning. In *Machine Learning for Engineers: Introduction to Physics-Informed, Explainable Learning Methods for AI in Engineering Applications* (pp. 141-172). Berlin, Heidelberg: Springer Berlin Heidelberg.
30. Noori, M., Vedaie, S. S., Singh, I., Crawford, D., Oberoi, J. S., Sanders, B. C., & Zahedinejad, E. (2020). Analog-quantum feature mapping for machine-learning applications. *Physical Review Applied*, *14*(3), 034034.
31. Nwadiugwu, M. C. (2020). Neural networks, artificial intelligence and the computational brain. *arXiv preprint arXiv:2101.08635*.
32. Ogwu, M. C. (2019). Towards sustainable development in Africa: the challenge of urbanization and climate change adaptation. *The geography of climate change adaptation in urban Africa*, 29-55.
33. Okhue, E. T., and Olorunfemi, M. O. (1991). Electrical resistivity investigation of a typical basement complex area-the Obafemi Awolowo University Campus case study. *Journal of Mining and Geology,* 27(2), Pp.63-69.
34. Olatokunbo-Ojo I. O. and Akintorinwa O. J. (2016). Hydrogeophysical Assessment of Aule Area, Akure Southwestern Nigeria. *Pacific Journal of Science and Technology*. 17(1):323-336.
35. Oloruntola, M. O., Folorunso, A. F., Bayewu, O. O., Mosuro, G. O., and Adewale, S. (2019). Baseline evaluation of freshwater–saltwater interface in coastal aquifers of Badagry, south-western Nigeria. *Journal of Applied water science*, 9(4), Pp.85.
36. Omeka, M. E. (2024). Evaluation and prediction of irrigation water quality of an agricultural district, SE Nigeria: An integrated heuristic GIS-based and machine learning approach. Environmental Science and Pollution Research, 31(41), 54178–54203. https://doi.org/10.1007/s11356-024-34162-2
37. Osman, A. I. A., Ahmed, A. N., Huang, Y. F., Kumar, P., Birima, A. H., Sherif, M., ... & El-Shafie, A. (2022). Past, present and perspective methodology for groundwater modeling-based machine learning approaches. *Archives of Computational Methods in Engineering*, *29*(6), 3843-3859.
38. Otchere, D. A., Ganat, T. O. A., Gholami, R., & Ridha, S. (2021). Application of supervised machine learning paradigms in the prediction of petroleum reservoir properties: Comparative analysis of ANN and SVM models. *Journal of Petroleum Science and Engineering*, *200*, 108182.
39. Priyan, K. (2021). Issues and challenges of groundwater and surface water management in semi-arid regions. In Groundwater resources development and planning in the semi-arid region (pp. 1–17).

40. Qader, S. H., Dash, J., Alegana, V. A., Khwarahm, N. R., Tatem, A. J., & Atkinson, P. M. (2021). The role of earth observation in achieving sustainable agricultural production in arid and semi-arid regions of the world. *Remote Sensing*, *13*(17), 3382.
41. Qamar, M. Z., Araib, T., Parveen, S., & Ali, W. (2021). Management of coastal aquifers with special reference to seawater intrusion and its remediation. *Management of Coastal Aquifers with special reference to seawater intrusion and its remediation*, *74*(1), 13-13.
42. Rahaman, M.A., Oluyide, P.O., Mbonu, W.C., Ogezi, A.E., Egbuniwe, I.G., Ajibade, A.C., Umeji, A.C., 1988. Recent advances in the study of the basement complex of Nigeria. In. Precambrian Geology of Nigeria. Geological Survey of Nigeria Special Publication 11, 41.
43. Rahimi, A., & Recht, B. (2007). Random Features for Large-Scale Kernel Machines. Advances in Neural Information Processing Systems (NIPS), 20, 1177-1184.
44. Rajabi, M. M., Ataie-Ashtiani, B., & Simmons, C. T. (2018). Model-data interaction in groundwater studies: Review of methods, applications and future directions. *Journal of hydrology*, *567*, 457-477.
45. Rajeev, A., Shah, R., Shah, P., Shah, M., & Nanavaty, R. (2025). The potential of big data and machine learning for ground water quality assessment and prediction. *Archives of Computational Methods in Engineering*, *32*(2), 927-941.
46. Rane, N., Choudhary, S., & Rane, J. (2024). Machine learning and deep learning: A comprehensive review on methods, techniques, applications, challenges, and future directions. *Techniques, Applications, Challenges, and Future Directions (May 31, 2024)*.
47. Raviraj, A., Kuruppath, N., and Kannan, B. (2017). Identification of potential groundwater recharge zones using remote sensing and geographical information system in Amaravathy basin. *J Remote Sens GIS,* 6(4), Pp.1-10.
48. Roy, D. K., Sarkar, T. K., Munmun, T. H., Paul, C. R., & Datta, B. (2025). A review on the applications of machine learning and deep learning to groundwater salinity modeling: present status, challenges, and future directions. *Discover Water*, *5*(1), 16.
49. Samadzadegan, F., Toosi, A., & Dadrass Javan, F. (2025). A critical review on multi-sensor and multi-platform remote sensing data fusion approaches: Current status and prospects. *International Journal of Remote Sensing, 46*(3), 1327–1402.
50. Saatsaz, M., and Eslamian, S. (2020). Groundwater modeling and its concepts, classifications, and applications for solute transport simulation in saturated porous media. *Advances in hydrogeochemistry research.*
51. Santos, C. F. G. D., & Papa, J. P. (2022). Avoiding overfitting: A survey on regularization methods for convolutional neural networks. *ACM Computing Surveys (Csur)*, *54*(10s), 1-25.
52. Shaikh, M., & Birajdar, F. (2024). Advancements in remote sensing and GIS for sustainable groundwater monitoring: applications, challenges, and future directions. *International Journal of Research in Engineering, Science and Management*, *7*(3), 16-24.
53. Singh, B., Kumar, R., & Singh, V. P. (2022). Reinforcement learning in robotic applications: a comprehensive survey. *Artificial Intelligence Review*, *55*(2), 945-990.
54. Singh, R., Anand, A. K., & Chattopadhyay, P. B. (2022). Investigation of topographical controls on the groundwater potential zone in a hilly watershed using a geospatial and

geophysical approach. *Water Resources Management, 36*(13), 5313–5333. https://doi.org/10.1007/s11269-022-03202-0
55. Srivastava, A., Saco, P. M., Rodriguez, J. F., Kumari, N., Chun, K. P., & Yetemen, O. (2021). The role of landscape morphology on soil moisture variability in semi-arid ecosystems. *Hydrological Processes, 35*(1), e13990. https://doi.org/10.1002/hyp.13990
56. Sun, D., Luo, N., Vandenhoff, A., McCall, W., Zhao, Z., Wang, C., … Illman, W. A. (2024). Evaluation of hydraulic conductivity estimates from various approaches with groundwater flow models. *Groundwater, 62*(3), 384–404. https://doi.org/10.1111/gwat.13373
57. Taye, M. M. (2023). Understanding of machine learning with deep learning: architectures, workflow, applications and future directions. *Computers*, *12*(5), 91.
58. Vohra, R., & Tiwari, K. C. (2020). Comparative analysis of SVM and ANN classifiers using multilevel fusion of multi-sensor data in urban land classification. *Sensing and Imaging*, *21*(1), 17.
59. Wali, S. U., Usman, A. A., & Usman, A. B. (2024). Resolving challenges of groundwater flow modelling for improved water resources management: a narrative review. *Int J Hydro*, *8*(5), 175-193.
60. Worqlul, A. W., Jeong, J., Dile, Y. T., Osorio, J., Schmitter, P., Gerik, T., ... & Clark, N. (2017). Assessing potential land suitable for surface irrigation using groundwater in Ethiopia. *Applied geography*, *85*, 1-13.
61. Yaseen, Z. M. (2023). A new benchmark on machine learning methodologies for hydrological processes modelling: A comprehensive review for limitations and future research directions. *Knowledge-Based Engineering and Sciences*, *4*(3), 65-103.
62. Yeboah-Forson, A., and Whitman, D. (2014). Electrical resistivity characterization of anisotropy in the Biscayne Aquifer. Groundwater, 52(5), Pp.728-736.
63. Zhou, X., Zhang, W., Chen, Z., Diao, S., & Zhang, T. (2021). Efficient neural network training via forward and backward propagation sparsification. *Advances in neural information processing systems*, *34*, 15216-15229.